Dariusz CHAŁADYNIAK*, Janusz M. JASIŃSKI
Military University of Technology, Faculty of Civil Engineering and Geodesy
S. Kaliskiego str. 2, 00-908 Warsaw, Poland
**Corresponding author*. E-mail: dchaladyniak@wat.edu.pl

INVESTIGATING ATMOSPHERIC INSTABILITIES POSING THREAT TO MARITIME NAVIGATION BY MEANS OF Q-VECTORS AND FRONTOGENETIC FUNCTION

Summary. Atmospheric instabilities, e.g. frontal zones with hazardous phenomena such as strong winds and intensive precipitation, pose threat to maritime activities including navigation. Capability to diagnose and forecast such processes may significantly reduce risk of casualties and damages to vessels or cargo. The paper presents a selected method of atmospheric instabilities analysis by means of mathematical and physical interpretation of the Q-vectors properties and their relation with the scalar frontogenetic function. A cartographic coordinate system for simultaneous analysis of GRID numerical data and satellite images - an aid developed for support of atmospheric instabilities investigation - is also presented.

BADANIE NIESTABILNOŚCI ATMOSFERYCZNYCH NIEBEZPIECZNYCH DLA ŻEGLUGI MORSKIEJ Z WYKORZYSTANIEM Q-WEKTORÓW I FUNKCJI FRONTOGENETYCZNEJ

Streszczenie. Niestabilności atmosferyczne, np. strefy frontów z niebezpiecznymi zjawiskami pogody, jak silny wiatr lub intensywne opady atmosferyczne, stanowią zagrożenie dla wszelkich działań na morzu, w tym dla żeglugi. Możliwości diagnozowania i prognozowania takich procesów mogą znacząco zmniejszyć ryzyko ofiar w ludziach i uszkodzeń statków lub ich ładunku. Artykuł przedstawia wybraną metodę analizy niestabilności atmosferycznych za pomocą matematycznej i fizycznej interpretacji własności Q-wektorów i ich relacji ze skalarną funkcją frontogenetyczną. Przedstawiono również kartograficzny układ współrzędnych do jednoczesnej analizy danych numerycznych GRID i zobrazowań satelitarnych – narzędzie opracowane w celu ułatwienia badania niestabilności atmosferycznych.

1. INTRODUCTION

The characteristics of frontogenetic function create a base for evaluation of conditions of fronts arising and formation. These characteristics are also expected to include clouds systems and atmospheric phenomena on the front. The characteristics are in use for forecasting the synoptical situation, which includes the expected location, evolution and movement of pressure systems, atmospheric fronts and characteristic of oncoming air masses. The method of Q-vectors used in this study is still unexplored in practice. The method has become a base of calculation of vertical movements, their sign and intensity. The areas of Q-vectors point the areas of convergence and divergence in the field of atmospheric flow, and thereby regions of ascending and descending air movements appearance. The calculation on their base frontogenetic function determines areas of frontogenesis and frontolysis. Its positive value means extension or origin of a new front system, the negative value – the front dissipation.

2. RELATIONS BETWEEN Q-VECTORS AND THE FRONTOGENETIC FUNCTION

The frontogenetic function is commonly used to investigate atmospheric instabilities, such as frontogenesis and frontolysis. It is a function that has only positive values for any arguments but its derivative with respect to time can have both positive and negative values. It is an example of so called Lapunov functions which are applied to investigate instabilities of numerous processes, including the atmospheric ones [4, 7].

The following forms for the frontogenetic function F_g concern 2D adiabatic geostrophic flow:

$$F_g = \frac{D_g}{Dt}|\nabla\theta| = \frac{\partial|\nabla\theta|}{\partial t} + u_g\frac{\partial|\nabla\theta|}{\partial x} + v_g\frac{\partial|\nabla\theta|}{\partial y}, \quad |\nabla\theta| = \sqrt{(\partial\theta/\partial x)^2 + (\partial\theta/\partial y)^2} \tag{1}$$

where: $D_g|\nabla\theta|/Dt$ - substantial derivative of the module of potential temperature gradient.

According to (1.1) the function F_g is a measure of the change of the module of potential temperature gradient of an individual air sample in geostrophic flow [4, 7].

Equation (1.1) may be rewritten in the following form:

$$\begin{aligned} F_g &= \frac{\partial\theta/\partial x}{|\nabla\theta|}\left(\frac{\partial^2\theta}{\partial t\partial x} + u_g\frac{\partial^2\theta}{\partial x^2} + v_g\frac{\partial^2\theta}{\partial x\partial y}\right) + \frac{\partial\theta/\partial y}{|\nabla\theta|}\left(\frac{\partial^2\theta}{\partial t\partial y} + u_g\frac{\partial^2\theta}{\partial x\partial y} + v_g\frac{\partial^2\theta}{\partial y^2}\right) = \\ &= \frac{\partial\theta/\partial x}{|\nabla\theta|}\left(\frac{\partial}{\partial x}\frac{D_g\theta}{Dt} - \frac{\partial u_g}{\partial x}\frac{\partial\theta}{\partial x} - \frac{\partial v_g}{\partial x}\frac{\partial\theta}{\partial y}\right) + \frac{\partial\theta/\partial y}{|\nabla\theta|}\left(\frac{\partial}{\partial y}\frac{D_g\theta}{Dt} - \frac{\partial u_g}{\partial y}\frac{\partial\theta}{\partial x} - \frac{\partial v_g}{\partial y}\frac{\partial\theta}{\partial y}\right) \end{aligned} \tag{2}$$

The form (1.2) indicates that the frontogenetic effects are caused by non-adiabatic processes, $D_g\theta/Dt \neq 0$, and by horizontal advection of inhomogeneous wind field.

In this case non-adiabatic processes are not considered and it is assumed that $D_g\theta/Dt=0$. It means that the frontogenetic effects are related with fields of the potential temperature gradient and geostrophic flow velocity. Substituting Q-vector components with:

$$\frac{D_g}{Dt}\left(f_0\frac{\partial u_g}{\partial p}\right) = -Q_2 \qquad \frac{D_g}{Dt}\left(f_0\frac{\partial v_g}{\partial p}\right) = +Q_1$$

the frontogenetic function F_g may be presented in the following form:

$$F_g = \frac{D_g}{Dt}|\nabla\theta| = \frac{\theta_0}{g\sqrt{(\partial\theta/\partial x)^2 + (\partial\theta/\partial y)^2}}\cdot\left(Q_1\cdot\partial\theta/\partial x + Q_2\cdot\partial\theta/\partial y\right) = \frac{\theta_0}{g}\frac{\nabla\theta\cdot\mathbf{Q}}{|\nabla\theta|} \tag{3}$$

The frontogenetic function determines regions where new frontal zones develop (frontogenesis) in areas where tendency for increasing the horizontal gradient of temperature is observed. In the opposite case old frontal zones dissipate (frontolysis). The following two figures present model cases of frontogenesis (Fig. 1a) and frontolysis (Fig. 1b) processes [4].

Fig. 1a presents a 2D model case of the frontogenesis process in which large scale geostrophic field increases the air temperature gradient. The circulation across the atmospheric frontal zone corresponds to a thermal vortex with ascending warm air and descending cold air. A clear geostrophic flow in the direction of the warm air mass is observed on a lower level of the atmosphere. In this case the Q-vectors are directed from the cold to the warm air mass.

In case of the frontolysis process (Fig. 1b) the large scale geostrophic field decreases the air temperature gradient. The Q-vectors are directed from the warm to the cold air mass. The circulation across the atmospheric frontal zone corresponds to a thermal vortex with ascending cold air and descending warm air [4].

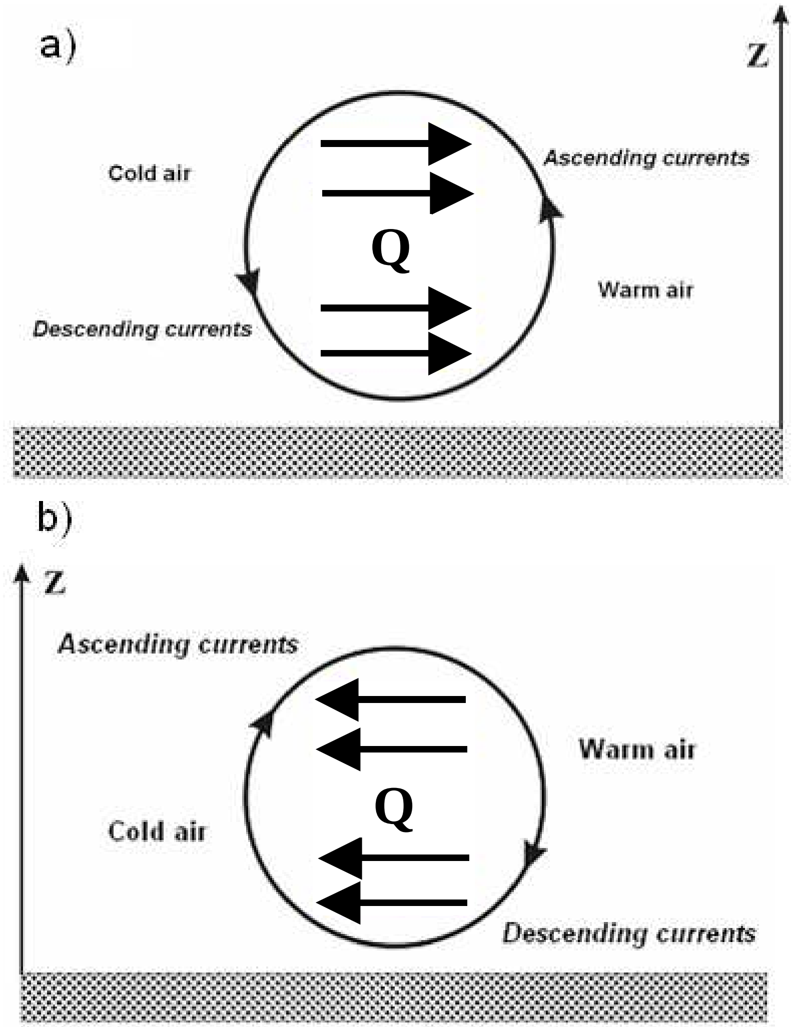

Fig. 1. a) 2D model case of the frontogenesis process (arrows depict Q-vectors); b) 2D model case of the frontolysis process (arrows depict Q-vectors). (B. J. Hoskins, M. A. Pedder, 1980)
Rys. 1. a) Dwuwymiarowy model procesu frontogenezy (strzałki wskazują Q-wektory); b) dwuwymiarowy model procesu frontolizy (strzałki wskazują Q-wektory). (B. J. Hoskins, M. A. Pedder, 1980)

3. A COORDINATE SYSTEM FOR SIMULTANEOUS ANALYSIS OF SATELLITE IMAGES AND GRID DATA

A common coordinate system is required for simultaneous analysis of satellite images and meteorological elements derived from GRID data. GRID data are provided in an angular grid of a spherical coordinate system while satellite images are a projection of atmospheric radiation onto a plane [1, 2, 3].

The analysis described above may be supported by means of a technology of superimposing meteorological information above geostationary satellite images which was developed in the Meteorology Section of the Military University of Technology. It enables to convert satellite images to numerous cartographic projections used in meteorology. The uniform angular cartographic projection was used for preparing data for this paper. In this case the relation necessary for calculations may be obtained by introducing an orthogonal coordinate system on a local f-plane, i.e. a plane that is tangential to the sphere at the point of (λ_0,φ_0) and rotating with the angular speed of the point - $\Omega\sin(\varphi_0)$ (Ω - speed of rotation of the Earth) [2, 6].

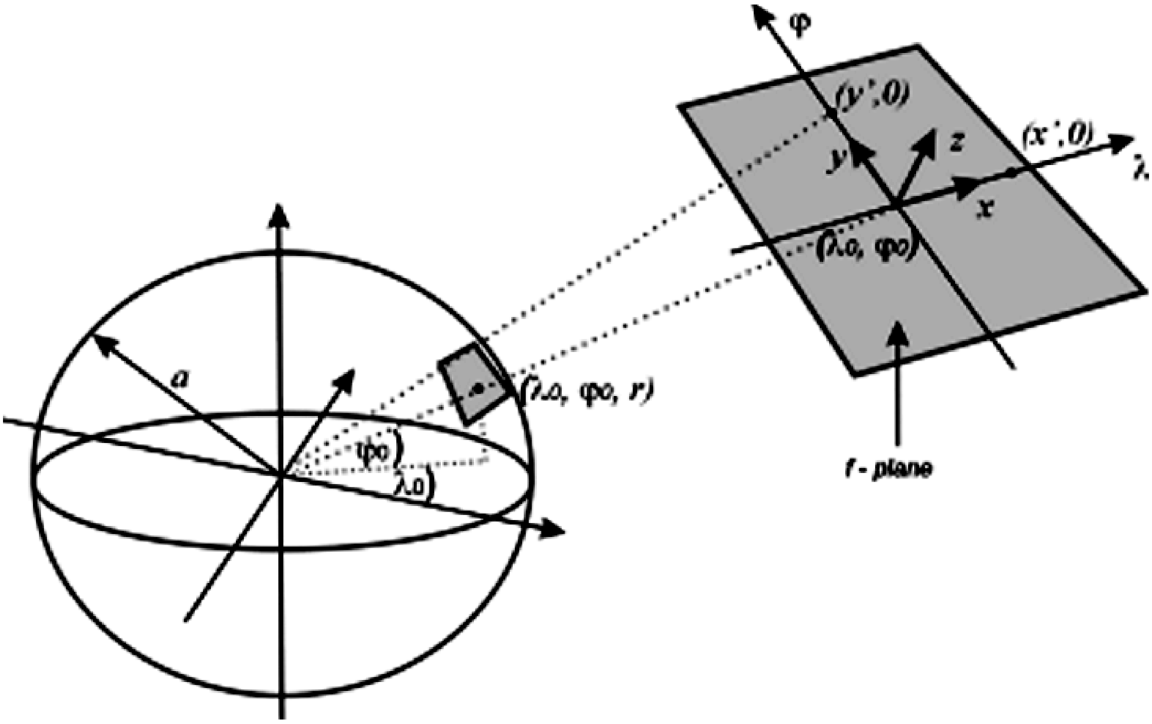

Fig. 2. Local orthogonal coordinate system for the f – plane. a – the sphere radius; (λ_0,φ_0) - geographical coordinates of a regular node of the GRID; (x, y) – the node's coordinates in the local system
(K. Kroszczyński, D. Chaładyniak, 1996)
Rys. 2. Lokalny prostokątny układ współrzędnych dla płaszczyzny f. a – promień sfery; (λ_0,φ_0) – współrzędne geograficzne węzła sieci GRID; (x, y) – współrzędne węzła w układzie lokalnym
(K. Kroszczyński, D. Chaładyniak, 1996)

To determine the components of the Q-vector in the local orthogonal coordinate system on the *f* – plane we use the following relations [6]:

$$\begin{cases} x = a\cdot\cos(\varphi_0)\cdot(\lambda-\lambda_0) \\ y = a\cdot(\varphi-\varphi_0) \end{cases} \Rightarrow \frac{\partial\lambda}{\partial y}=\frac{\partial\varphi}{\partial x}=0,\quad \frac{\partial\lambda}{\partial x}=\frac{1}{a\cdot\cos(\varphi_0)},\quad \frac{\partial\varphi}{\partial y}=\frac{1}{a} \tag{4}$$

Hence:

$$\begin{cases} \dfrac{\partial\theta}{\partial x}=\dfrac{\partial\theta}{\partial\lambda}\cdot\dfrac{\partial\lambda}{\partial x}+\dfrac{\partial\theta}{\partial\varphi}\cdot\dfrac{\partial\varphi}{\partial x}=\dfrac{1}{a\cdot\cos(\varphi_0)}\cdot\dfrac{\partial\theta}{\partial\lambda} \\ \dfrac{\partial\theta}{\partial y}=\dfrac{\partial\theta}{\partial\lambda}\cdot\dfrac{\partial\lambda}{\partial y}+\dfrac{\partial\theta}{\partial\varphi}\cdot\dfrac{\partial\varphi}{\partial y}=\dfrac{1}{a}\cdot\dfrac{\partial\theta}{\partial\varphi} \end{cases} \tag{5}$$

and:

$$\frac{\partial u_g}{\partial z}\cdot\frac{\partial v_g}{\partial x}+\frac{\partial v_g}{\partial z}\cdot\frac{\partial v_g}{\partial y}=\frac{-g}{\theta_o f}\left[\frac{\partial u_g}{\partial x}\cdot\frac{\partial\theta}{\partial x}+\frac{\partial v_g}{\partial x}\cdot\frac{\partial\theta}{\partial y}\right]=-\frac{g}{\theta_o}\left(\frac{\partial(u_g,v_g)}{\partial x}\cdot\nabla\theta\right)=\frac{1}{f}\cdot Q_1$$
$$\frac{\partial u_g}{\partial z}\cdot\frac{\partial u_g}{\partial x}+\frac{\partial v_g}{\partial z}\cdot\frac{\partial u_g}{\partial y}=\frac{g}{\theta_o f}\left[\frac{\partial u_g}{\partial y}\cdot\frac{\partial\theta}{\partial x}+\frac{\partial v_g}{\partial y}\cdot\frac{\partial\theta}{\partial y}\right]=\frac{g}{\theta_o}\left(\frac{\partial(u_g,v_g)}{\partial y}\cdot\nabla\theta\right)=-\frac{1}{f}\cdot Q_2 \tag{6}$$

Finally:

$$Q_\lambda=-\frac{g}{\theta_o}\left(\frac{1}{a^2\cos^2(\varphi)}\frac{\partial u_g}{\partial\lambda}\frac{\partial\theta}{\partial\lambda}+\frac{1}{a^2\cos(\varphi)}\frac{\partial v_g}{\partial\lambda}\frac{\partial\theta}{\partial\varphi}\right)=-\frac{g}{\theta_o\cdot a\cdot\cos(\varphi)}\left(\frac{\partial(u_g,v_g)}{\partial\lambda}\cdot\nabla\theta\right) \tag{7}$$

$$Q_\varphi=-\frac{g}{\theta_o}\left(\frac{1}{a^2\cos(\varphi)}\frac{\partial u_g}{\partial\varphi}\frac{\partial\theta}{\partial\lambda}+\frac{1}{a^2}\frac{\partial v_g}{\partial\varphi}\frac{\partial\theta}{\partial\varphi}\right)=-\frac{g}{\theta_o\cdot a}\left(\frac{\partial(u_g,v_g)}{\partial\varphi}\cdot\nabla\theta\right) \tag{8}$$

In the forms above, the $\cos(\varphi_0)$ was replaced with $\cos(\varphi)$ because the Q-vector components are calculated for each node of the regular angular GRID in the corresponding local orthogonal coordinate system [6]. The scalar frontogenetic function has the following form:

$$\frac{D_g}{Dt}|\nabla\theta|=\frac{\theta_0}{g\sqrt{\frac{1}{\cos^2\varphi}(\partial\theta/\partial x)^2+(\partial\theta/\partial y)^2}}\cdot\left(\frac{1}{\cos\varphi}\frac{\partial\theta}{\partial x}Q_\lambda+\frac{\partial\theta}{\partial y}Q_\varphi\right)=\frac{\theta_0}{g}\frac{\nabla_s\theta\cdot\mathbf{Q}}{|\nabla_s\theta|} \tag{9}$$

where: ∇_s - operator in the spherical coordinate system

4. CONCLUSIONS

Current meteorological data availability and accessibility e.g. over the Internet networks enable to use the presented method of atmospheric instabilities analysis for diagnosing areas of phenomena posing threat to maritime activities including navigation. Increasing computing power of personal computers makes it possible to apply the developed software for cartographic coordinate systems conversions in an 'on-line' mode in order to obtain numerical data and satellite images for simultaneous analysis. The method enables to estimate areas of ascending and descending air currents; creation and development of cyclonic and anticyclonic systems including areas of frontogenesis and frontolysis with high accuracy providing capability to reduce risk of casualties and damages to vessels or cargo by proper route planning and monitoring.

Bibliography

1. Chaładyniak D.: *Analysis of cloud systems by means of Q-vector fields and satellite images*, 31st Conference on Broadcast Meteorology, Williamsburg, Virginia, 2002.
2. Chaładyniak D.: *Wybrane metody teledetekcyjne i numeryczne w prognozowaniu procesów frontogenezy i frontolizy*, Rozprawa doktorska, Warszawa, 2002.
3. Chaładyniak D.: *Analysis and forecasting of frontogenesis and frontolysis processes by means of Q-vectors method*, XIV-th International Scientific and Technical Conference, The Part of Navigation in Support of Human Activity on the Sea, Gdynia, 2004.
4. Hoskins B. J., Pedder M. A.: *The diagnosis of middle latitude synoptic development*, Quart. J. Roy. Meteorol. Soc., vol. 106, 1980, p. 707-719.

5. Jasiński J. M.: *Dynamiczny wskaźnik frontogenezy*, Ogólnopolskie Sympozjum z Meteorologii Wojskowej, WAT-WLOP, Warszawa, 21-23.03.1996, s. 27-43.
6. Jasiński J., Kroszczyński K., Pietrek S., Trześniak W.: *Meteosat satellite images transformation to UMPL mesoscale model projection*, V Międzynarodowe Sympozjum z Meteorologii Wojskowej "Zadania służb meteorologicznych i oceanograficznych (METOC) w operacjach, misjach i ćwiczeniach prowadzonych przez NATO", Poznań-Kiekrz, 29.09 – 2.10.2003.
7. Sanders F., Hoskins B. J.: *An easy method for estimation of Q-vectors from weather maps*, Weather Forecasting, vol. 5, No. 2, 1990, p. 346-353.

Received 28.04.2008; accepted in revised form 10.06.2008